Front. Optoelectron. 2014, 7(3): 348–358
DOI 10.1007/s12200-014-0449-8

REVIEW ARTICLE

Carrier recovery in coherent receiver of optical orthogonal frequency division multiplexing system

Changyuan YU (✉)[1,2], Pooi-Yuen KAM[1], Shengjiao CAO[2]

1 Department of Electrical and Computer Engineering, National University of Singapore, Singapore 117576, Singapore
2 A*STAR Institute for Infocomm Research (I2R), Singapore 138632, Singapore

Abstract In this paper, we reviewed our common phase error (CPE) and intercarrier interference (ICI) compensation methods for coherent optical orthogonal frequency division multiplexing (CO-OFDM) system. We first presented a unified CPE estimation framework combining decision-aided (DA), pilot-aided (PA) and decision feedback (DF) algorithms. The DA method is used to estimate the CPE of the current OFDM symbol based on the decision statistics of the previous symbol. DA + PA helps increase the phase noise tolerance of DA and reduce the overhead of PA, while DA + DF reduces the overhead to zero, achieving best performance with one more step of estimation, compensation and demodulation. We also described a modified time-domain blind intercarrier interference (BL-ICI) mitigation algorithm over non-constant amplitude formats. The new algorithm is derived from the BL-ICI algorithm over constant amplitude format for wireless networks. A new power estimation scheme was proposed for the BL-ICI algorithm to adapt to non-constant amplitude format. It has the same order of complexity with frequency domain decision-aided ICI (DA-ICI) compensation method and does not suffer from symbol decision errors. The effectiveness of both CPE and ICI compensation algorithms were demonstrated in a simulated 56-Gbit/s CO-OFDM system with various modulation formats.

Keywords linear phase noise, coherent optical orthogonal frequency division multiplexing (CO-OFDM), common phase error (CPE), decision-aided (DA), intercarrier interference (ICI)

Received May 31, 2014; accepted June 16, 2014

E-mail: eleyc@nus.edu.sg

1 Introduction

Coherent optical orthogonal frequency division multiplexing (CO-OFDM) offers advantages such as its dispersion tolerance, ease of frequency domain equalization and high spectral efficiency [1]. Several experiments on CO-OFDM transmission [2–4] have proved it as a suitable candidate for the 100 Gb/s Ethernet transport. Moreover, several 1 Tb/s and beyond (per channel) CO-OFDM experiments have been carried out in Refs. [5–8].

One of the major challenges in coherent detection is to overcome carrier phase noise when using a local oscillator (LO) to beat with received signals to retrieve modulated information. Carrier phase noise is generated by both transmitter laser and receiver local oscillators. An optical phase-locked loop (PLL) is one solution to track the carrier phase with respect to the LO carrier in early days of coherent optical communication. However, an optical PLL operating at optical wavelengths in combination with distributed feedback lasers is quite difficult to implement [9]. With the availability of high-speed analog-to-digital converters (ADCs), the carrier phase estimation can be done in high-speed digital signal processing (DSP) units rather than using an optical PLL for carrier phase tracking, allowing for free-running LO laser [10]. Due to its longer symbol duration, OFDM is more sensitive to linear phase noise compared to a single carrier system. Moreover, as the OFDM symbol is modulated in the frequency domain, algorithms like M-th power cannot be applied in the time domain before Fast Fourier transform (FFT). Uncompensated phase noise will cause common phase error (CPE) and intercarrier interference (ICI) to the received signal after FFT. Thus, a compensation method before FFT is preferred as it allows removing ICI. Works in Refs. [11–13] showed inserting an unmodulated RF-pilot tone in the middle of the OFDM band and a guard band around it provides the required reference for phase estimation and compensation. In this case, the power allocated to the pilot

tone must be carefully selected with a tradeoff between phase estimation accuracy and energy wasted for pilot tone. Alternatively, phase estimation can be done in the frequency domain after the FFT block. In this case, compensation works include CPE compensation only [14–17] or CPE + ICI compensation methods [18–24] with much higher computational complexity.

The CPE compensation methods can be categorized into two groups: pilot-subcarrier aided (PA) and decision-feedback (DF) methods. A PA phase compensation method is first introduced in Refs. [14,15], it estimates the CPE based on a few pilot-subcarriers inserted into the OFDM spectrum. DF methods have also been proposed in the literatures [15,18,19]. The proposed decision-directed phase estimation (DDPE) method in Refs. [18,19] uses the initial decisions of the current symbol to re-estimate the phase noise, re-compensate and demodulate again, which involves two steps of estimation, compensation and demodulation. Thus, the DDPE method is more computationally intensive than the pilot-tone or pilot-subcarrier aided method, yet it suffers from decision errors as it is purely decision directed.

However, the correction of the CPE does not always suffice, especially for larger laser linewidth and higher-order modulation format. Methods have been proposed to estimate the higher spectral components of phase noise thus reducing ICI in either wireless [18–20] or optical [21–24] domain. Works presented in Refs. [18,19,21] compensate for CPE using pilots and make hard decisions first. In Ref. [24], the authors proposed to replace the pilots in Ref. [21] with pseudo-pilots to achieve higher spectral efficiency. ICI is then estimated based on the initial decisions, which will suffer from falsely detected symbols. In Ref. [23], the researcher discards pilots and estimates both CPE and ICI in a decision-aided manner by running multiple iterations. Those decision-aided ICI (DA-ICI) compensation methods will suffer from decision errors, resulting in performance degradation. The matched filtering approach in Ref. [22] uses adaptive equalization based on an FIR filter which cancels the phase noise. However, it requires as many as $2N$ (N is the DFT size) iterations to converge and the calculation also involves decision statistics. A blind ICI compensation scheme over constant amplitude modulation was proposed in Ref. [20] for wireless communication. The authors partitioned one received OFDM symbol into sub blocks and used the approximate average phase noise over each sub block to cancel ICI.

In this paper, we reviewed our proposed algorithms for combating both CPE [25,26] and ICI [27]. We first presented a unified CPE compensation framework [26], which combines PA, decision-aided (DA) [25] and DF algorithms. The DA method was initially proposed for the single carrier system [28,29], which estimates the CPE of the current symbol from the decisions of the previous symbols. We compared the efficiency and effectiveness of PA, DA, DF methods and their combinations in a simulated 56-Gb/s back-to-back CO-OFDM system. The combination of DA and PA is shown to improve phase noise tolerance compared to DA while reducing overhead compared to PA. The combination of DA and DF offers better tolerance to linear phase noise compared to DA and other purely decision-directed methods.

We also presented a modified time-domain blind ICI (BL-ICI) mitigation method for non-constant amplitude modulation format, e.g., M-QAM [27]. To calculate the actual signal power in BL-ICI algorithm, we proposed three schemes: 1) use the average power; 2) use the approximate power; 3) use the average power for 1st iteration and approximate power for 2nd iteration. The modified algorithm was demonstrated to be effective in mitigating ICI for a simulated 56-Gb/s CO-OFDM system over various non-constant amplitude modulation formats: 8-QAM, 16-QAM, 32-QAM and 64-QAM. Furthermore, it shows superior performance with the same complexity compared to DA-ICI compensation algorithm at larger laser linewidth, especially for higher-order modulation format.

In reduced guard-interval (RGI) CO-OFDM systems, different subcarriers will experience different phase rotations because of local oscillator laser phase noise and the relatively large walk-off between subcarriers. References [30,31] investigate and compensate for this dispersion-enhanced phase noise (DEPN) effects in RGI CO-OFDM system. However, this effect is negligible in conventional CO-OFDM systems as the symbol duration is much longer than the dispersion induced walk-off. Thus, we did not deal with DEPN effects in our investigated conventional CO-OFDM system.

2 System model

Figure 1 shows the simulation model of our CO-OFDM system. We denote by $X_{k,i}$, the frequency-domain complex modulation symbol associated to the k-th subcarrier and i-th OFDM symbol, with $k = 0,1,...,N-1$. The discrete time-domain samples are obtained by discrete Fourier transform (DFT):

$$x_{N*i+n} = \frac{1}{N}\sum_{k=0}^{N-1} X_{k,i} e^{j2\pi kn/N}. \quad (1)$$

With perfect window and frequency synchronization, the received OFDM signal y_n at sampling time instant nT_s is expressed as

$$y_n = e^{j\phi_n}\sum_{l=0}^{L-1} h_l x_{n-l} + w_n, \quad (2)$$

where x_n, y_n, h_n and w_n denote the transmitted signal, received signal, channel impulse response and additive

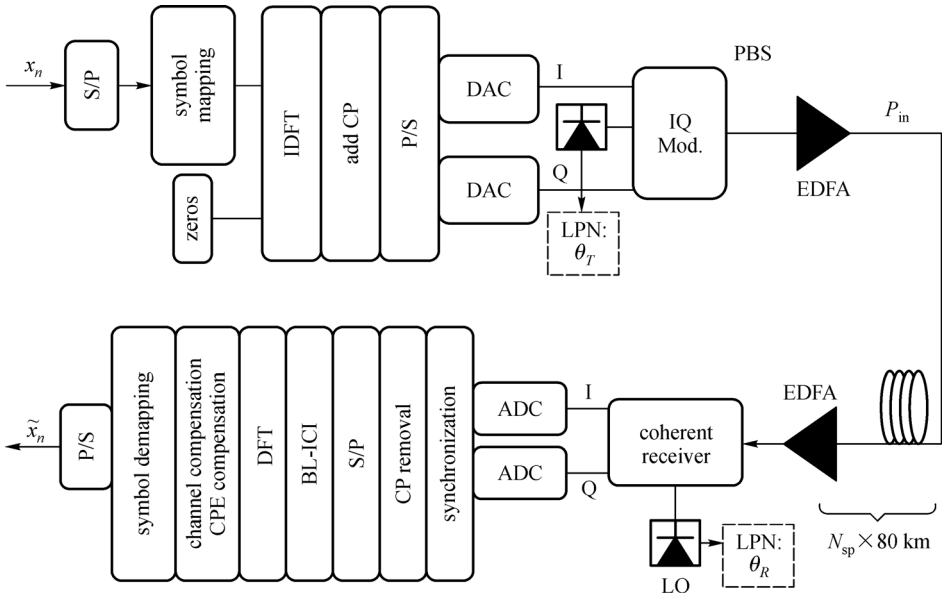

Fig. 1 Simulation setup for coherent optical orthogonal frequency division multiplexing (CO-OFDM) system. S/P: serial to parallel; P/S: parallel to serial; DAC: digital to analog converter; ADC: analog to digital converter; Mod.: modulator; EDFA: erbium doped fiber amplifier

white Gaussian noise (AWGN), respectively. The linear phase noise ϕ_n is a Wiener-Levy process described by $\phi_{n+1} = \phi_n + \Delta\phi_n$, where $\Delta\phi_n$ is a set of independent and identically distributed, zero-mean Gaussian random variables, each with variance of $\sigma^2 = 2\pi\nu T_s$. ν is the combined laser linewidth. After removing cyclic prefix and taking N-point FFT, the resulting frequency domain signal is given by

$$Y_{k,i} = I_{0,i}H_kX_{k,i} + \sum_{l=0,l\neq k}^{N-1} I_{k-l,i}H_lX_{l,i} + W_{k,i}, \tag{3}$$

$$I_{m,i} = \frac{1}{N}\sum_{n=0}^{N-1} e^{j\phi_{n,i}}e^{-j2\pi mn/N}, \tag{4}$$

where $X_{k,i}$, $Y_{k,i}$, H_k and $W_{k,i}$ are the frequency domain representations of x_n, y_n, h_n and w_n, respectively. The time subscript i in $H_{k,i}$ is dropped as channel distortion that could be considered constant throughout a certain OFDM window. The term $I_{0,i}$ could be written as $|I_{0,i}|e^{j\Phi_i}$, where Φ_i is defined as CPE for i-th symbol. The second additive term in Eq. (4) is defined as ICI. Assuming the channel distortion is removed first based on preambles as in Refs. [14,32], the simplified model becomes

$$\hat{Y}_{k,i} = |I_{0,i}|e^{j\Phi_i}X_{k,i} + \sum_{l=0,l\neq k}^{N-1} I_{k-l,i}X_{l,i} + W_{k,i}. \tag{5}$$

3 Methodology: CPE compensation

In this section, we only compensate for CPE by assuming that the ICI term is approximated as AWGN and $|I_{0,i}| \approx 1$.

$$\hat{Y}_{k,i} = e^{j\Phi_i}X_{k,i} + W'_{k,i}, \tag{6}$$

where $W'_{k,i}$ includes both AWGN ($W_{k,i}$) and ICI term. Similar to the single carrier case in Ref. [29], we introduce a complex phasor V^{DA} based on the decision statistics of previous symbols for M-ary phase shift keying (PSK) OFDM system:

$$V_{k,i}^{DA} = \sum_{j=i-L}^{i-1} \hat{Y}_{k,j}D^*_{k,j}, \tag{7}$$

where $D_{k,j}$ is the receiver's decision for the symbol $Y_{k,j}$, and L is defined as the memory length. Because the phase rotation is common for different subcarriers, we can get a more accurate phase reference V_i by averaging across all the subcarriers. Due to the longer symbol duration in OFDM than in single carrier case, the optimum memory length L is found to be 1. The DA phasor for M-ary PSK OFDM system is defined as

$$V_i^{DA} = \frac{1}{N}\sum_{k=0}^{N-1} \hat{Y}_{k,i-1}D^*_{k,i-1}. \tag{8}$$

Similar to the DA method, we define a new phasor V^{PA} based on the pilot subcarriers for the PA method:

$$V_i^{\mathrm{PA}} = \frac{1}{N_{\mathrm{p}}} \sum_{k=0}^{N_{\mathrm{p}}-1} \hat{Y}_{k,i} X_{k,i}^*, \tag{9}$$

where N_{p} is the number of pilot subcarrers. To combine the DA and PA method, we define $V^{\mathrm{DA+PA}}$ as the weighted sum of V^{DA} and V^{PA}:

$$V_i^{\mathrm{DA+PA}} = \gamma V_i^{\mathrm{DA}} + (1-\gamma) V_i^{\mathrm{PA}}, \tag{10}$$

where γ is the weight factor defined over (0,1). Thus, CPE is estimated from the complex phasors as

$$\hat{\Phi}_i = \begin{cases} \angle V^{\mathrm{DA}}, & \mathrm{DA\ method}, \\ \angle V^{\mathrm{PA}}, & \mathrm{PA\ method}, \\ \angle V^{\mathrm{DA+PA}}, & \mathrm{DA+PA\ method}. \end{cases} \tag{11}$$

A decision-feedback stage is added after DA, PA or DA + PA method with one extra step of residual phase noise estimation, compensation and demodulation. Figure 2 shows the combined phase estimation scheme of DA, PA and DF.

Different from M-ary PSK system, the DA and PA phasors are normalized by the energy of the decisions for M-QAM system:

$$V_i^{\mathrm{DA}} = \frac{1}{N} \sum_{k=0}^{N-1} \left| D_{k,i-1} \right|^{-2} \hat{Y}_{k,i-1} D_{k,i-1}^*, \tag{12}$$

$$V_i^{\mathrm{PA}} = \frac{1}{N_{\mathrm{p}}} \sum_{k=0}^{N_{\mathrm{p}}-1} \left| X_{k,i} \right|^{-2} \hat{Y}_{k,i} X_{k,i}^*. \tag{13}$$

Table 1 compares the computational complexity of different methods by listing the number of complex multiplications and demodulation times. From the table, we can sort the methods from the most computationally intensive to least intensive as: DDPE > DA + DF > DA + PA > DA > PA.

4 Methodology: ICI compensation

In this section, we will introduce our blind ICI mitigation algorithm for CO-OFDM systems over non-constant amplitude modulation format, e.g., 16-QAM [27]. As given by Eq. (5), the frequency-domain received signal is

$$\hat{Y}_k = I_0 X_k + \sum_{l=0, l\neq k}^{N-1} I_{k-l} X_l + W_k,$$

omitting the time subscript. One received OFDM symbol is partitioned into N_{B} subblocks with equal length $S = N/N_{\mathrm{B}}$ in the time-domain, while the time-average of the phase noise at each subblock is defined as $\overline{\phi}_q (0 \leqslant q \leqslant N_{\mathrm{B}} - 1)$. In the high signal-to-noise (SNR) region, a relation between the squared magnitude of the channel gain multiplied by

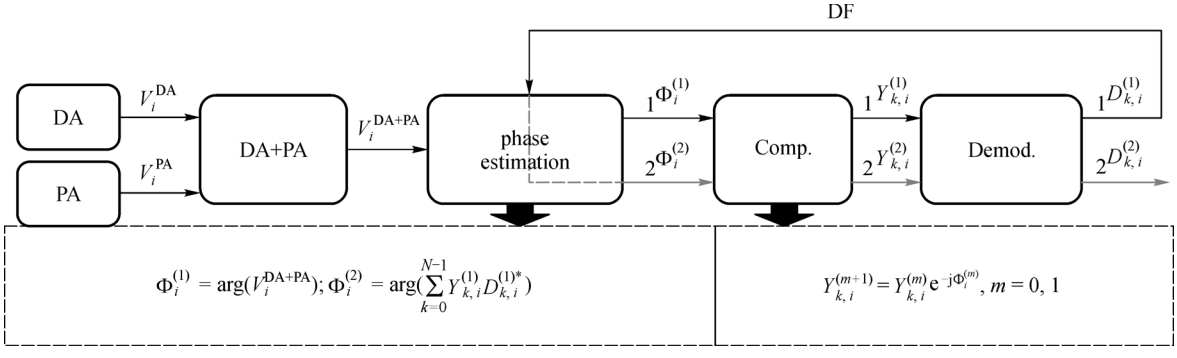

Fig. 2 Phase estimation algorithm of DA + PA ($D_{k,i}^{(1)}$,0<γ<1), DA + DF ($D_{k,i}^{(2)}$,γ = 1), PA + DF ($D_{k,i}^{(2)}$,γ = 0) and DA + PA + DF ($D_{k,i}^{(2)}$,0<γ<1) (Comp: compensation; Demod: demodulation)

Table 1 Complexity comparison of different methods: DA [25,26], PA [14], DA + PA [26], DA + DF [26] and DDPE [17]

method	complex multiplications for phase estimation	complex multiplications for phase compensation	total complex multiplications	demodulation
DA	N	N	$2N$	1 time
PA	N_{p}	N	$N + N_{\mathrm{p}}$	1 time
DA + PA	$N + N_{\mathrm{p}}$	N	$2N + N_{\mathrm{p}}$	1 time
DA + DF	$2N$	$2N$	$4N$	2 times
DDPE	$3N$	$2N$	$5N$	2 times

the data symbol and the time averages $\overline{\phi}_q$ can be established as follows [20]:

$$|H_k|^2|X_k|^2 = \left|\sum_{q=0}^{N_B-1}\exp(-j\overline{\phi}_q)\exp\left(-j\frac{2\pi qSk}{N}C_{k,q}\right)\right|^2, \tag{14}$$

where $C_{k,q}$ is the N-point DFT of the received samples at the qth subblock with zero padding. For constant amplitude modulation, e.g., M-ary PSK, a constant signal power E_x is assigned to $|X_k|^2$ [20]. To extend the blind estimation method to non-constant amplitude modulation format, e.g., 16-QAM, we assign $E_k = |X_k|^2$ with either the average signal power equal to E_s or approximate signal power equal to R_i^2 where $i = \arg\min_j \left||Y_k|^2 - R_j^2\right|$. As depicted in Fig. 3, each received symbol Y_k can be approximately located on one of the three rings from 16-QAM constellation, and its approximate power equals the squared ring radius. Exploiting the relationship in Eq. (14), the blind ICI mitigator then calculates the differences $d_q = \overline{\phi}_q - \overline{\phi}_0$ by [20]

$$\hat{\boldsymbol{d}} = \left[\hat{d}_1, \hat{d}_2, ..., \hat{d}_{N_B-1}\right]^T = (\boldsymbol{A}^T\boldsymbol{A})^{-1}\boldsymbol{A}^T\boldsymbol{r}, \tag{15}$$

$$r_k = |H_k|^2 E_k - \sum_{q=0}^{N_B-1}|C_{k,q}|^2 - 2\sum_{q_1=0}^{N_B-1}\sum_{q_2=q_1+1}^{N_B-1}|C_{k,q_1}||C_{k,q_2}|\cos(\theta_{k,q_1,q_2}), \tag{16}$$

$$A_{m,n} = 2\left\{\sum_{q=n+2}^{N_B-1}|C_{m,n+1}||C_{m,q}|\sin(\theta_{m,n+1,q}) - \sum_{q=0}^{n}|C_{m,n+1}||C_{m,q}|\sin(\theta_{m,q,n+1})\right\}, \tag{17}$$

where $A_{m,n}$ is the (m,n) th entry of matrix $\boldsymbol{A}$ and $\theta_{k,q_1,q_2} = \angle C_{k,q_1} - \angle C_{k,q_2} + 2\pi(q_2 - q_1)Sk/N$. To further improve the performance, we could run two iterations of the algorithm (Eq. (15)) using average power for the 1st iteration and approximate power for the 2nd iteration. After ICI compensation in the time domain, the pilot-subcarrier aided (PA) method [14] is applied to remove the CPE in the frequency domain.

5 Simulation results

We simulated a CO-OFDM system based on the setup in Fig. 1 using MATLAB. The original 56-Gbit/s data are modulated onto 640 subcarriers with QPSK (or 16-QAM, 64-QAM) modulation, which, together with N_p pilot subcarriers, are transferred to the time domain with a FFT/IFFT size of 1024. The other subcarriers are zero padded for oversampling purpose and the filling ratio is 62.5%. A cyclic prefix of 256 samples is added to each symbol, resulting in an OFDM symbol size of 1280 samples. The discrete samples are converted to real-time waveform by 56-Gsample/s or 28-Gsample/s or ~19-Gsample/s DAC for QPSK or 16-QAM or 64-QAM, respectively. Each OFDM frame consists of 20 payload symbols and 2 training symbols. The given laser linewidth value is single laser linewidth for both Tx and Rx laser and the combined laser linewidth would be double of the value given.

5.1 CPE compensation

In the first part of simulation, we demonstrated the performance of our unified CPE compensation framework, which combines DA, PA and DF algorithms. In this case, we only consider linear phase noise and back-to-back transmission. DDPE [17], which is a purely decision directed scheme, is included for comparison with our unified CPE compensation framework. γ (for both DA + PA and DDPE) is optimized for each data point by sweeping over all possible values from 0 to 1 with a step-size of 0.1.

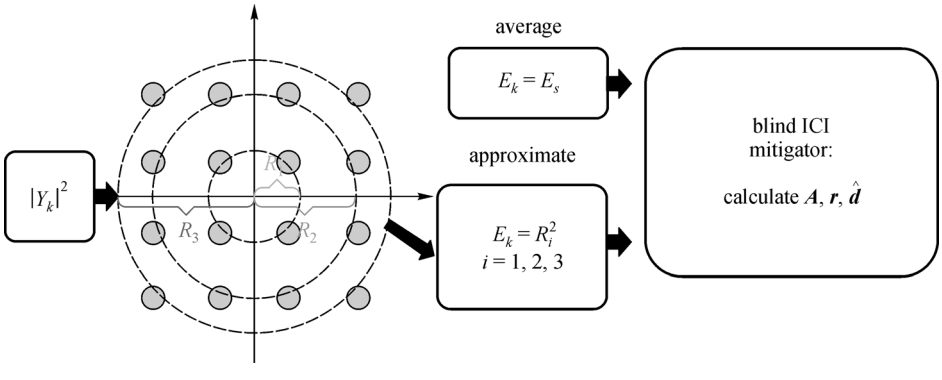

Fig. 3 Blind ICI mitigation algorithm for non-constant amplitude format using average signal power or approximate signal power

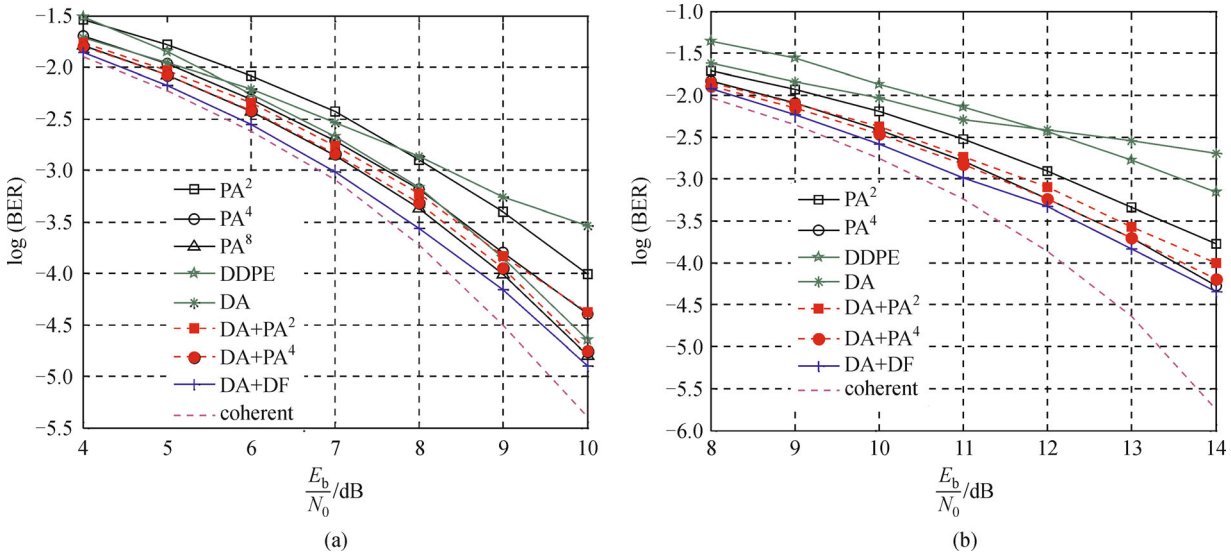

Fig. 4 BER curves of PA$^{2/4/8}$, DDPE, DA, DA + PA$^{2/4}$, DA + DF and coherent (no phase noise) for (a) QPSK, 100-kHz laser linewidth; (b) 16-QAM, 20-kHz laser linewidth

Figure 4(a) shows the BER performance versus the effective energy per bit to noise power spectral density ratio (E_b/N_0) for 100-kHz (QPSK) laser linewidth in the case of PA$^{2/4}$, DDPE, DA, DA + PA$^{2/4}$ and DA + DF. PA^n means PA with n pilot subcarriers. The coherent case (with no linear phase noise) is plotted as baseline for comparison, which always performs the best. DA + PA with 2 (or 4) pilot subcarriers require almost the same E_b/N_0 as PA with 4 (or 8) pilot subcarriers to achieve a BER value of 10^{-3}, while the overhead is reduced by 50%. Moreover, the performance of PA/DA/(DA + PA) in combination with DF converges to the same BER curve, which is the best among all. Thus, we only consider DA + DF because it has zero overhead.

Figure 4(b) plots the BER versus effective E_b/N_0 for 16-QAM signal with 20-kHz laser linewidth. With the same bit rate, 16-QAM CO-OFDM is less tolerant to laser linewidth than its QPSK counterpart (Fig. 4(a)), due to its longer symbol duration and denser constellation diagram.

To investigate the required number of pilot subcarriers N_p for both PA and DA + PA method, we plot the total E_b/N_0 (BER = 10^{-3} or 10^{-4}) against N_p in Fig. 5(a) for QPSK with 100-kHz laser linewidth. We define the effective $\mathrm{SNR_b}$ as the average signal energy over N_0 while the total $\mathrm{SNR_b}$ is defined as the average of the signal energy and pilot-subcarrier energy per bit over N_0. The total $\mathrm{SNR_b}$ takes the overhead introduced by pilot-subcarrier into consideration:

$$\{E_b/N_0\}_{\mathrm{total}}[\mathrm{dB}] = 10\log_{10}[1 + N_p/N_{\mathrm{data}}] + \{E_b/N_0\}_{\mathrm{eff}}[\mathrm{dB}].$$

DA + PA reduces the total required E_b/N_0 significantly when the number of pilot subcarriers is small. For example, DA + PA$^{2/4}$ requires almost the same E_b/N_0 as PA$^{4/8}$.

Figure 5(b) shows the total required E_b/N_0 (BER = 10^{-3}) of PA$^{2/4/8}$, DDPE, DA, DA + PA$^{2/4}$ and DA + DF against laser linewidth for QPSK. DDPE and DA fail to achieve BER of 10^{-3} within 10-dB E_b/N_0 when the laser linewidth is beyond 120 kHz due to error propagation. Our proposed DA + DF performs best and is more tolerant to phase noise than DDPE with the same overhead and lower complexity. This is because the filtering window for phase noise in DA + DF is smaller than DDPE. DA + PA^2 (or DA + PA^4) requires almost the same or even less E_b/N_0 than PA^4 (or PA^8) for $v < 120$ kHz. The required E_b/N_0 of DA increases quickly as the laser linewidth increases. This is because the phase variance between consecutive OFDM symbols ($\sigma^2 = 2\pi vt$) will increase with the increase of laser linewidth. And the reliability of V^{DA}, which is calculated from the previous OFDM symbol, will decrease. Thus, DA is performing better with smaller laser linewith.

5.2 Blind ICI compensation

In this section, we will evaluate the performance of our BL-ICI algorithm for 16-QAM CO-OFDM system. Six pilot subcarriers are inserted for CPE compensation. A frequency-domain decision-aided ICI (DA-ICI) mitigation method [18,19] is included for comparison. Compared to the method employed in Refs. [18,19], the optical methods in Refs. [21,23,24] are based on the same frequency-domain model and follow quite similar procedure by calculating the ICI components up to a degree L using hard decisions. Thus, we only compare our time-domain BL-ICI mitigation algorithm with one implementation of the frequency-domain method for simplicity. Table 2 lists the computational complexity comparison between BL-ICI

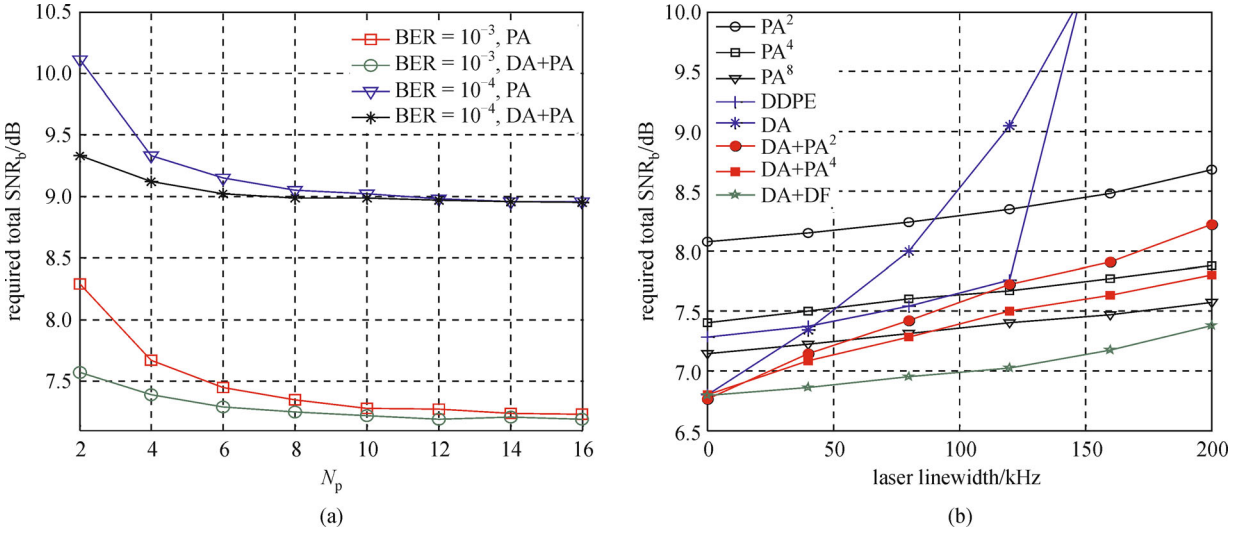

Fig. 5 (a) Required total E_b/N_0 value at BER = 10^{-3} or 10^{-4} versus N_p of PA and DA + PA method for 100-kHz laser linewidth (QPSK); (b) required total E_b/N_0 of $PA^{2/4/8}$, DDEP, DA, DA + $PA^{2/4}$ and DA + DF versus laser linewidth (QPSK)

Table 2 Computational complexity comparison between BL-ICI (average) and DA-ICI

	BL-ICI (average)	DA-ICI
N-point DFT	$N_B + 1$	1
demodulation	1	2
matrix inversion	$(N_B-1)\times(N_B-1)$	$(2u+1)\times(2u+1)$

(average) and DA-ICI. As matrix inversion is the most complex operation ($O(L^3)$), we conclude that BL-ICI (average) and DA-ICI have the same order of complexity with $N_B - 1 = 2u + 1$. Note that BL-ICI (2 iterations) needs two times of operation for N-point DFT and matrix inversion as compared to BL-ICI (average).

Figure 6 shows the approximation on a realization of the phase noise for different knowledge of E_k: (a) perfect, (b) average, (c) approximate and (d) 2 iterations. The perfect knowledge case treated the transmitted symbol as known and is shown as an upper limit of performance. As depicted by the figure, both average and approximate cases can greatly remove ICI while the two iterations case is almost as good as the perfect case.

In the first case, back-to-back system was simulated. In Fig. 7(a), the required effective E_b/N_0 versus laser linewidth curves (BER = 10^{-3}) are plotted using different knowledge of E_k in 16-QAM CO-OFDM system. For laser linewidth beyond 50 kHz, approximate result becomes worse than average result, because lager laser phase noise will introduce larger ICI, which makes the approximate result less accurate. However, running two iterations will greatly improve the performance as approximate results are much closer to the actual power waveform at 2nd iteration. It is observed that the 2 iterations method exhibits less than 0.5-dB SNR_b penalty compared to the perfect case, for laser linewidth smaller than 300 kHz. Figure 7(b) shows the BER performance of different M-QAM formats at 100-kHz laser linewidth. 2Iter-BL-ICI and Avg-BL-ICI achieve the best and second best performance among the three methods for higher-order modulation formats (16-QAM to 64-QAM).

In the second case, we simulated 2-span transmission of 80-km SSMF (attenuation: 0.2 dB/km, dispersion: 17 ps/nm/km, nonlinear coefficient: 0 $W^{-1}\cdot km^{-1}$) and EDFA (noise figure = 6 dB) without optical dispersion compensation for 16-QAM and 64-QAM. Laser phase noise is added at both transmitter and receiver. We implemented the intra-symbol frequency-domain averaging based channel estimation [32]. The parameters for both algorithms (N_B, u) are set to (4, 1) such that DA-ICI and Avg-BL-ICI share the same order of complexity and further increasing N_B or u will not noticeably improve the performance under current circumstances. Figures 8(a) and 8(b) shows the required OSNR versus laser linewidth using different methods: PA CPE compensation only, DA-ICI and BL-ICI with average power for 16-QAM (BER = 10^{-3}) and 64-QAM (BER = 3.8×10^{-3}, 7% FEC threshold), respectively. DA-ICI performs slightly better than our BL-ICI for $v < 120$ kHz (or 40 kHz), yet it suffers from an error floor and fails to reach the required BER beyond 200 kHz (or 60 kHz) laser linewidth for 16-QAM (or 64-QAM). From Fig. 8, we

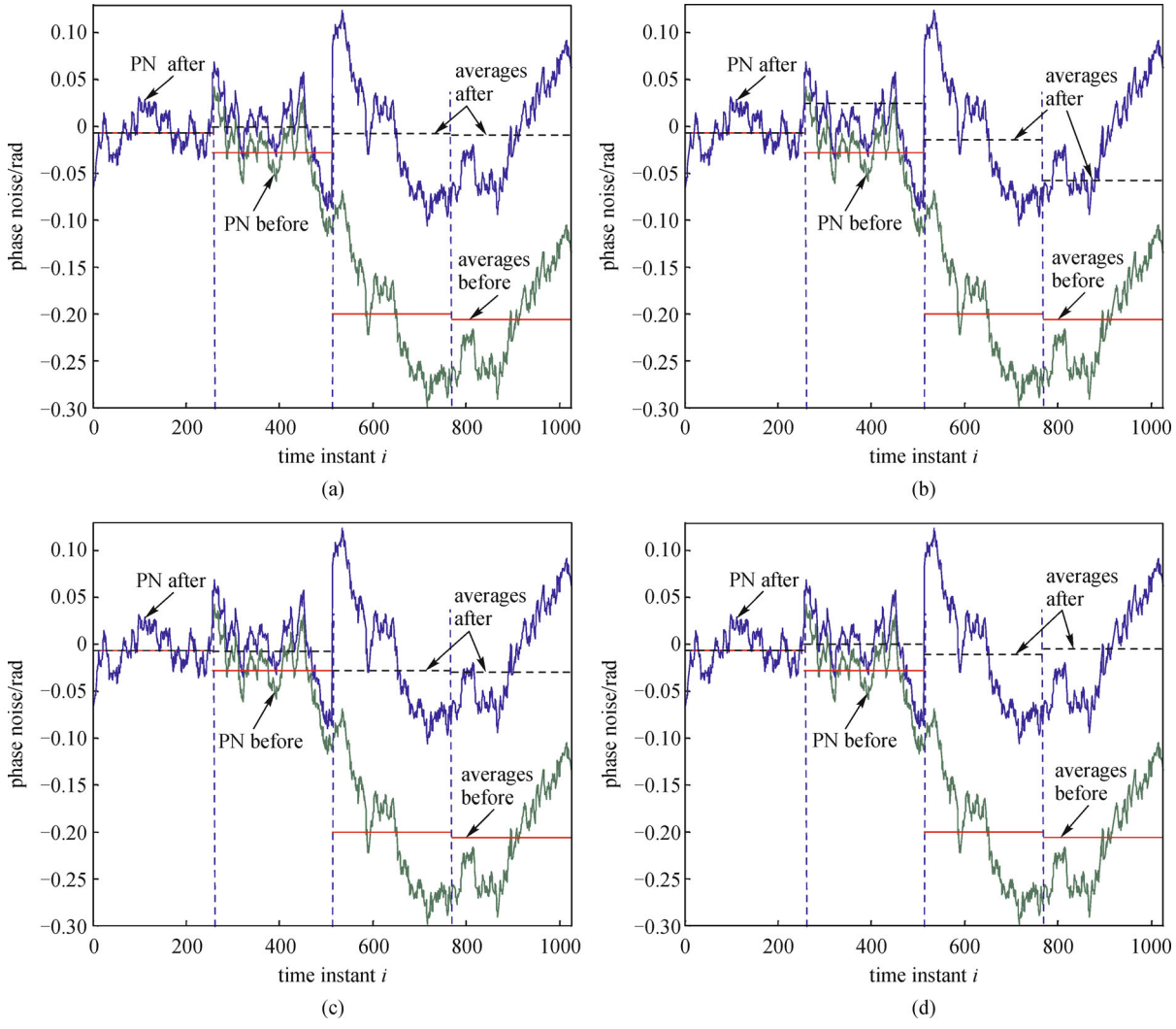

Fig. 6 Phase noise realization and its time-averages over the subblocks before (phase noise: green solid, average: red solid) and after (phase noise: blue solid, average: black dashed) ICI compensation when v = 100 kHz for different knowledge of E_k: (a) perfect, (b) average, (c) approximate and (d) 2 iterations

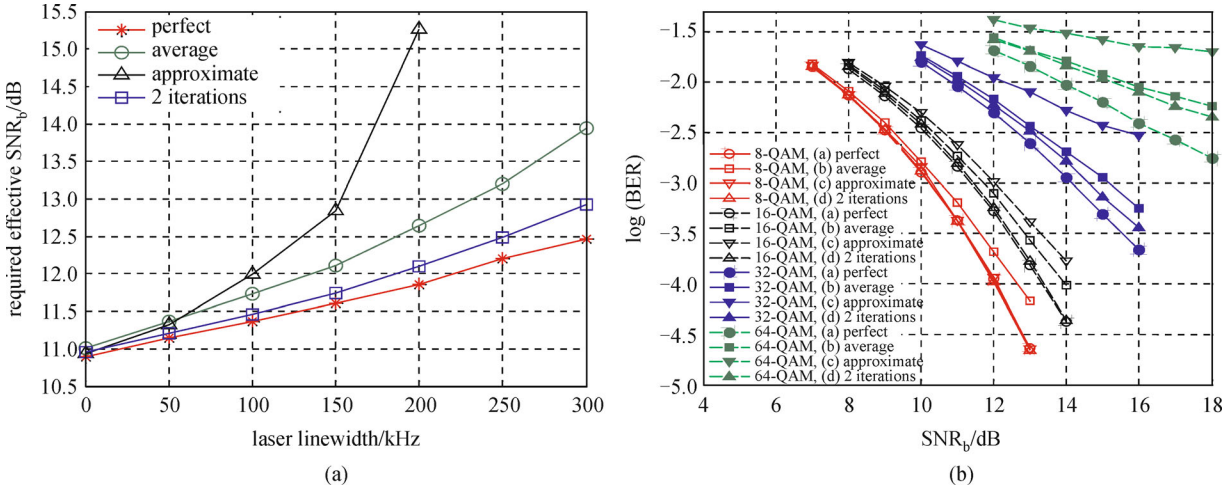

Fig. 7 (a) Required effective SNR_b versus laser linewidth for back-to-back 16-QAM CO-OFDM system using different knowledge of E_k; (b) BER versus SNR_b with different knowledge of E_k at 100-kHz laser linewidth for different modulation formats: M-QAM (M = 8, 16, 32, 64)

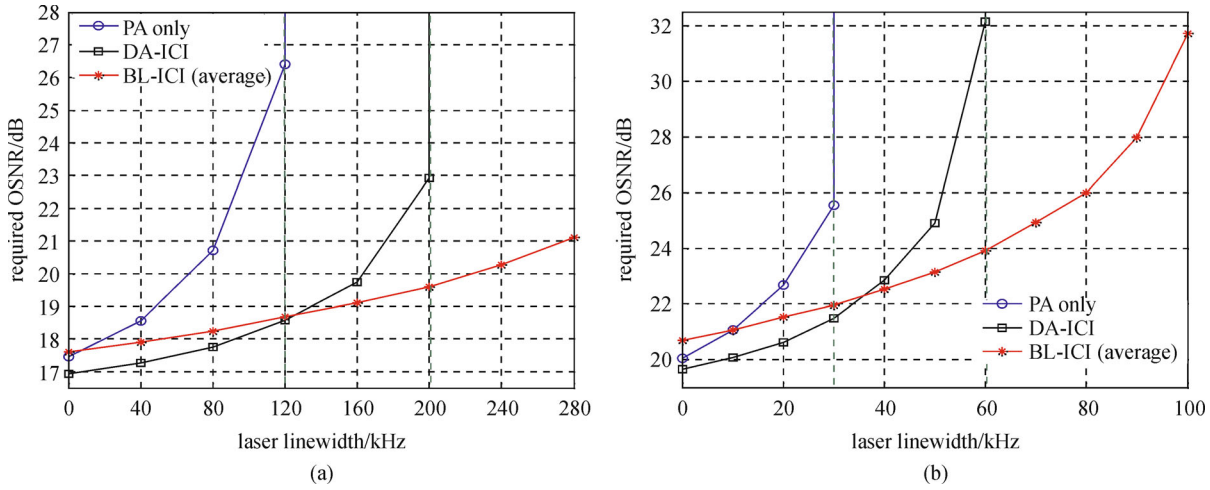

Fig. 8 Required OSNR versus laser linewidth after 2-span transmission for (a) 16-QAM (BER = 10^{-3}) and (b) 64-QAM (BER = 3.8×10^{-3}) OFDM using PA CPE compensation only, DA-ICI and BL-ICI with average signal power

conclude that our time-domain BL-ICI method with average power is performing better compared with frequency-domain DA-ICI at larger laser linewidth, especially for higher-order modulation format. This is because in DA-ICI, the estimation of higher spectral components will suffer from falsely detected symbols, especially for larger laser linewidth or higher-order modulation format.

6 Conclusions

In this paper, we presented carrier recovery algorithms in coherent receiver of optical OFDM system. We reviewed our compensation algorithms for two effects caused by linear phase noise in CO-OFDM system: common phase error and intercarrier interference. We first presented a unified CPE compensation framework, which combines pilot-aided, decision-aided and decision-feedback methods. Furthermore, we presented our modified time-domain blind ICI mitigation algorithm for non-constant amplitude modulation formats. New power estimation methods were introduced for the BL-ICI algorithm to adapt to non-constant amplitude modulation formats in CO-OFDM system.

The effectiveness of both CPE and ICI compensation methods were demonstrated in a simulated 56-Gb/s CO-OFDM system with various formats. DA + PA is able to reduce the overhead of PA while improve the phase noise tolerance of DA. DA + DF was demonstrated to be performing the best among all the phase estimation schemes with zero overhead. The modified BL-ICI algorithm was demonstrated to be effective in mitigating ICI over various non-constant amplitude modulation formats: 8-QAM, 16-QAM, 32-QAM and 64-QAM. Furthermore, it showed superior performance with the same complexity compared to the decision-aided ICI compensation algorithm at larger laser linewidth, especially for higher-order modulation format.

Acknowledgements The authors would like to thank the support of AcRF Tier 2 Grant MOE2013-T2-2-145 from MOE Singapore.

References

1. Shieh W, Djordjevic I. OFDM for Optical Communications. Burlington: Academic Press, 2009
2. Shieh W, Yang Q, Ma Y. 107 Gb/s coherent optical OFDM transmission over 1000-km SSMF fiber using orthogonal band multiplexing. Optics Express, 2008, 16(9): 6378–6386
3. Hobayash T, Sano A, Yamada E. Electro-optically subcarrier multiplexed 110 Gb/s OFDM signal transmission over 80 km SMF without dispersion compensation. Electronics Letters, 2008, 44(3): 225–226
4. Jansen S L, Morita I, Tanaka H. 10 × 121.9-Gb/s PDM-OFDM transmission with 2-b/s/Hz spectral efficiency over 1000 km of SSMF. In: Proceedings of Optical Fiber Communication Conference, 2008
5. Yi X W, Fontaine N K, Scott R P, Yoo S. Tb/s coherent optical OFDM systems enabled by optical frequency combs. Journal of Lightwave Technology, 2010, 28(14): 2054–2061
6. Hillerkuss D, Schellinger T, Schmogrow R, Winter M, Vallaitis T, Bonk R, Marculescu A, Li J, Dreschmann M, Meyer J, Ben Ezra S, Narkiss N, Nebendahl B, Parmigiani F, Petropoulos P, Resan B, Weingarten K, Ellermeyer T, Lutz J, Moller M, Huebner M, Becker J, Koos C, Freude W, Leuthold J. Single source optical OFDM transmitter and optical FFT receiver demonstrated at line rates of 5.4 and 10.8 Tbit/s. In: Proceedings of Optical Fiber Communication Conference, 2010
7. Ma Y R, Yang Q, Tang Y, Chen S M, Shieh W. 1-Tb/s single-channel coherent optical OFDM transmission with orthogonal-band

multiplexing and subwavelength bandwidth access. Journal of Lightwave Technology, 2010, 28(4): 308–315
8. Yu J, Dong Z, Xiao X, Xia Y. Generation, transmission and coherent detection of 11.2 Tb/s (112×100Gb/s) single source optical OFDM superchannel. In: Proceedings of Optical Fiber Communication Conference, 2011
9. Noe R. PLL-free synchronous QPSK polarization multiplex/diversity receiver concept with digital I & Q baseband processing. IEEE Photonics Technology Letters, 2005, 17(4): 887–889
10. Pfau T, Hoffmann S, Peveling R, Bhandare S, Ibrahim S K, Adamczyk O, Porrmann M, Noe R, Ac Y. First real-time data recovery for synchronous QPSK transmission with standard DFB lasers. IEEE Photonics Technology Letters, 2006, 18(18): 1907–1909
11. Jansen S L, Morita I, Takeda N, Tanaka H. 20-Gb/s OFDM transmission over 4160-km SSMF enabled by RF-pilot tone phase noise compensation. In: Proceedings of Optical Fiber Communication Conference, 2007
12. Jansen S L, Morita I, Schenk T, Takeda N, Tanaka H. Coherent optical 25.8-Gb/s OFDM transmission over 4160-km SSMF. Journal of Lightwave Technology, 2008, 26(1): 6–15
13. Randel S, Adhikari S, Jansen S. Analysis of RF-pilot-based phase noise compensation for coherent optical OFDM systems. IEEE Photonics Technology Letters, 2010, 22(17): 1288–1290
14. Yi X, Shieh W, Tang Y. Phase estimation for coherent optical OFDM. IEEE Photonics Technology Letters, 2007, 19(12): 919–921
15. Shieh W. Maximum-likelihood phase estimation and channel estimation for coherent optical OFDM. IEEE Photonics Technology Letters, 2008, 20(8): 605–607
16. Mousa-Pasandi M E, Plant D V. Data-aided adaptive weighted channel equalizer for coherent optical OFDM. Optics Express, 2010, 18(4): 3919–3927
17. Mousa-Pasandi M E, Plant D V. Zero-overhead phase noise compensation via decision-directed phase equalizer for coherent optical OFDM. Optics Express, 2010, 18(20): 20651–20660
18. Petrovic D, Rave W, Fettweis G. Phase noise suppression in OFDM including intercarrier interference. In: Proceedings of International OFDM Workshop (InOWo), 2003
19. Petrovic D, Rave W, Fettweis G. Intercarrier interference due to phase noise in OFDM - estimation and suppression. In: Proceedings of Vehicular Technology Conference (VTC), 2004
20. Lee M, Lim S, Yang K. Blind compensation for phase noise in OFDM systems over constant modulus modulation. IEEE Transactions on Communications, 2012, 60(3): 620–625
21. Yang C, Yang F, Wang Z. Orthogonal basis expansion-based phase noise estimation and suppression for CO-OFDM systems. IEEE Photonics Technology Letters, 2010, 22(1): 51–53
22. Chung W. A matched filtering approach for phase noise suppression in CO-OFDM systems. IEEE Photonics Technology Letters, 2010, 22(24): 1802–1804
23. Lin C T, Wei C C, Chao M I. Phase noise suppression of optical OFDM signals in 60-GHz RoF transmission system. Optics Express, 2011, 19(11): 10423–10428
24. Zhao C, Yang C, Yang F, Zhang F, Chen Z. A CO-OFDM system with almost blind phase noise suppression. IEEE Photonics Technology Letters, 2013, 25(17): 1723–1726
25. Cao S, Kam P Y, Yu C. Decision-aided carrier phase estimation for coherent optical OFDM. In: Proceedings of Opto-Electronics and Communications Conference (OECC), 2011
26. Cao S, Kam P Y, Yu C. Decision-aided, pilot-aided, decision-feedback phase estimation for coherent optical OFDM systems. IEEE Photonics Technology Letters, 2012, 24(22): 2067–2069
27. Cao S, Kam P, Yu C. Time-domain blind ICI mitigation for non-constant modulus format in CO-OFDM. IEEE Photonics Technology Letters, 2013, 25(24): 2490–2493
28. Zhang S, Kam P Y, Chen J, Yu C. Decision-aided maximum likelihood detection in coherent optical phase-shift-keying system. Optics Express, 2009, 17(2): 703–715
29. Zhang S, Kam P Y, Yu C, Chen J. Decision-aided carrier phase estimation for coherent optical communications. Journal of Lightwave Technology, 2010, 28(11): 1597–1607
30. Zhuge Q, Morsy-Osman M H, Plant D V. Low overhead intra-symbol carrier phase recovery for reduced-guard-interval CO-OFDM. Journal of Lightwave Technology, 2013, 31(8): 1158–1169
31. Zhuge Q, Chen C, Plant D V. Dispersion-enhanced phase noise effects on reduced-guard-interval CO-OFDM transmission. Optics Express, 2011, 19(5): 4472–4484
32. Liu X, Buchali F. Intra-symbol frequency-domain averaging based channel estimation for coherent optical OFDM. Optics Express, 2008, 16(26): 21944–21957

Changyuan Yu has been an assistant professor at Department of Electrical and Computer Engineering, National University of Singapore since 12/2005. He is also a 25% joint senior scientist with A*STAR Institute for Infocomm Research. He received the B.S. degree in applied physics and B. Economics degree in management from Tsinghua University, China in 1997, the M.S. degree in electrical and computer engineering from the University of Miami, USA in 1999, and the Ph.D. degree in electrical engineering from the University of Southern California, USA in 2005. He was a visiting researcher at NEC Labs America in 2005. His research focuses on photonic devices, subsystems, and optical fiber communication and sensor systems. Dr. Yu has authored/co-authored 6 book chapters and over 200 research papers on the peer reviewed journals and the prestigious conferences (32 invited). He has served in technical program committee or organizing committee for over 40 international conferences. He won IEEE/LEOS Graduate Student Fellowship Award in 2004.

Pooi-Yuen Kam was born in Ipoh, Malaysia, and educated at the Massachusetts Institute of Technology, Cambridge, Mass., USA, where he obtained the S.B., S.M., and Ph.D. degrees in electrical engineering in 1972, 1973, and 1976, respectively. From 1976 to 1978, he was a member of the technical staff at the Bell Telephone Laboratories, Holmdel, N.J.,

USA, where he was engaged in packet network studies. Since 1978, he has been with the Department of Electrical and Computer Engineering, National University of Singapore, where he is now a professor. He served as the Deputy Dean of Engineering and the Vice Dean for Academic Affairs, Faculty of Engineering of the National University of Singapore, from 2000 to 2003. His research interests are in the communication sciences and information theory, and their applications to wireless and optical communications. He spent the sabbatical year 1987 to 1988 at the Tokyo Institute of Technology, Tokyo, Japan, under the sponsorship of the Hitachi Scholarship Foundation. In 2006, he was invited to the School of Engineering Science, Simon Fraser University, Burnaby, B.C., Canada, as the David Bested Fellow.

Dr. Kam is a member of Eta Kappa Nu, Tau Beta Pi, and Sigma Xi. Since September 2011, he is a senior editor of the IEEE Wireless Communications Letters. From 1996 to 2011, he served as the Editor for Modulation and Detection for Wireless Systems of the IEEE Transactions on Communications. He also served on the editorial board of PHYCOM, the Journal of Physical Communications of Elsevier, from 2007 to 2012. He was elected a Fellow of the IEEE for his contributions to receiver design and performance analysis for wireless communications. He received the Best Paper Award at the IEEE VTC2004-Fall, at the IEEE VTC2011-Spring, and at the IEEE ICC2011.

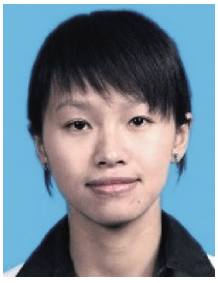

Shengjiao Cao has been working in A*STAR Institute of Inforcomm Research, Singapore since 3/2014. She received the B. E. degree in Department of Automation from Tsinghua University, China in 2009 and the Ph.D. degree in electrical and computer engineering from National University of Singapore in 2014. Her research interests include digital signal processing and LDPC codes for coherent optical OFDM system.